1 of 1

CONF-940103--2

SIMULATION AND PERFORMANCE COMPARISON OF LiBr/H_2O TRIPLE-EFFECT ABSORPTION CYCLES

R. C. DeVault
G. Grossman*
M. Wilk*

*Technion-Israel Institute of Technology

January 1994

submitted to
1994 International Absorption Conference

Prepared by the
OAK RIDGE NATIONAL LABORATORY
managed by
MARTIN MARIETTA ENERGY SYSTEMS, INC.
Oak Ridge, Tennessee 37831-2008
for the
U.S. DEPARTMENT OF ENERGY
under Contract No. DE-AC05-84OR21400

DISCLAIMER

This report was prepared as an account of work sponsored by an agency of the United States Government. Neither the United States Government nor any agency thereof, nor any of their employees, makes any warranty, express or implied, or assumes any legal liability or responsibility for the accuracy, completeness, or usefulness of any information, apparatus, product, or process disclosed, or represents that its use would not infringe privately owned rights. Reference herein to any specific commercial product, process, or service by trade name, trademark, manufacturer, or otherwise does not necessarily constitute or imply its endorsement, recommendation, or favoring by the United States Government or any agency thereof. The views and opinions of authors expressed herein do not necessarily state or reflect those of the United States Government or any agency thereof.

MASTER

DISTRIBUTION OF THIS DOCUMENT IS UNLIMITED

Simulation and Performance Comparison of LiBr/H_2O Triple-Effect Absorption Cycles

by

R.C. DeVault*, G. Grossman** and M. Wilk**

* Energy Division, Oak Ridge National Laboratory, Oak Ridge, Tennessee 37831, USA

** Faculty of Mechanical Engineering, Technion-Israel Institute of Technology, Haifa 32000, Israel

ABSTRACT

Performance simulation has been carried out for several LiBr/H2O triple-effect cycles using the Absorption Simulation Model (ABSIM). The systems investigated include the three-condenser-three-desorber (3C3D) cycle, forming an extension of the conventional double-effect cycle; and two cycles which additionally recover heat from the hot condensate leaving the highest temperature condenser by adding the heat to the lowest temperature desorber. These latter two cycles are called Double Condenser Coupled (DCC) cycles since each uses heat recovered from the highest temperature refrigerant to heat both the middle temperature desorber (heat of condensation) and the lowest temperature desorber (by further subcooling the condensed refrigerant), hence the "double-coupling".

ABSIM, A modular computer code for simulation of absorption systems, was used to investigate the performances of each of the cycles and compare them on an equivalent basis. The performance simulation was carried out over a range of operating conditions, including some investigation into the influence of varying particular design parameters. Cooling coefficients of performance ranging from 1.27 for the series-flow 3C3D to 1.73 for the parallel-flow DCC have been calculated at the design point. Relative merits of these LiBr/H2O triple-effect cycle configurations are discussed.

LIST OF SYMBOLS AND ABBREVIATIONS

3C3D - Three-Condenser-Three-Desorber triple-effect
CAT - Closest Approach Temperature
CFC's - Chloro-Fluoro-Carbon refrigerants
COP - Coefficient Of Performance
Desorber - Generator (the terms are used interchangeably)
DCC - Double-Condenser-Coupled triple-effect cycle
DCCA - Double-Condenser-Coupled-Alternate triple-effect cycle
First Generator - The lowest temperature and pressure generator equivalent to a single-effect generator
First Condenser - The lowest temperature and pressure condenser equivalent to a single-effect condenser
GAX - Generator-Absorber heat eXchange
Generator - Desorber (the terms are used interchangeably)
PTX - Pressure-Temperature-liquid composition
SAM-15 - Solar Absorption Machine, 15 refrigeration tons capacity
Second Generator - The middle generator in a triple-effect cycle, equivalent to a double-effect temperature and pressure
Second Condenser - The middle condenser in a triple-effect cycle, equivalent to a double-effect temperature and pressure
TH - Temperature of solution leaving the externally heated, gas-fired desorber, characterizing the heat supply temperature.(e.g. T_{37} in Figures 5-9)
TC - Cooling water supply (inlet) temperature (e.g. T_3 and T_{23} in Figures 5-9)
Third Generator - The highest temperature and pressure generator added to achieve triple-effect
Third Condenser - The highest temperature and pressure condenser added to achieve triple-effect
UA - overall heat transfer coefficient times area

INTRODUCTION

Concerns about the environmental effects of CFCs, electric capacity shortages during periods of peak load, and the substantially increased cost of building new electric power plants have generated renewed and growing interest in gas-fired absorption chillers. The last decade has seen intensive research and development efforts on advanced absorption cycles and systems for both heating and cooling applications in the USA, Europe and Japan.

Virtually all current gas-fired absorption cooling systems are based on the well-known single-effect or double-effect cycles. Generally, all small air-cooled absorption cooling systems use ammonia as the refrigerant with water as the absorbent (NH3/H2O); and large commercial chiller systems use water as the refrigerant with lithium bromide as the absorbent (LiBr/H2O).

Single effect commercial chillers (COP=~0.5-0.7) are limited in their ability to utilize high temperature heat sources, and are particularly suitable for waste heat or solar applications. Double-effect chillers (COP=~0.9-1.2+) represent a significant step in performance improvement over the basic single-effect cycle. Triple-effect chiller cycles are theoretically capable of substantial performance improvement over equivalent double-effect cycles. A variety of triple-effect cycles are currently being developed throughout the world.

Many triple-effect cycles are theoretically possible (Alefeld, 1982,1983a,1983b,1985a,1985b,1993; Zeigler, 1985,1987,1993; Devault, 1988,1989,1990a,1990b,1992a,1992b; Miyoshi, 1985; Oouchi, 1985). Many triple-effect cycles require the use of absorption fluids with wide solubility fields. A relatively small number of the possible triple-effect cycles are feasible using LiBr/H2O because of crystallization limits. This paper focuses on specific triple-effect chiller cycles using only the conventional LiBr/H2O absorption fluids.

LiBr/H2O TRIPLE-EFFECT CHILLER CYCLES

The first LiBr/H2O double-effect chiller was experimentally built and operated by J.S. Swearingen and E.P. Whitlow in 1956-1959 at Southwest Research Institute (Whitlow, 1958,1993). This double-effect cycle added a second high-temperature desorber and condenser to the basic single-effect cycle, using heat rejected from the high-temperature condenser for heating the low-temperature desorber. After further development, the double-effect cycle first demonstrated by Swearingen/Whitlow was commercialized. Over the past decades, this basic condenser-coupled double-effect cycle has been extensively improved, principally by Japanese manufacturers. In particular, Japanese manufacturers introduced direct-fired double-effect chillers (the original double-effects were steam-fired) and parallel solution flow (originally series

flow)(Kurosawa, 1988). Today, the Japanese "Ultra-efficiency" double-effect chillers are thought to be, for all practical purposes, at the efficiency limit for commercially manufacturable heat exchangers (Wilkinson, 1987).

While building the first double-effect chiller prototype in 1956-1959, Swearingen and Whitlow considered building a triple-effect by "doing it again" (eg: adding a third condenser and desorber to the double-effect) (Whitlow, 1993). The first double-effect prototype experienced several development problems, in particular substantially increased corrosion encountered in the high temperature double-effect generator. Whitlow states that they decided that the generator temperature needed for the triple-effect would be "too high", so they did not try to build such a machine in 1956-1959. The basic three-condenser-three-desorber (3C3D) triple-effect cycle has since been patented (Oouchi et al, 1985) and the "PTX" diagram is shown in Figure 1.

For convenience, the highest temperature and highest pressure desorber (generator) and condenser needed to achieve the triple-effect are named the third desorber and third condenser. The middle temperature and pressure desorber and condenser, equivalent to those of a double-effect, are named the second desorber and second condenser. Likewise, the lowest temperature and pressure desorber and condenser are named the first desorber and first condenser. The refrigerant flows from each generator and condenser are named, respectively, the third, second, and first refrigerant flow.

Further performance improvements are possible by adding additional heat exchange features to the basic 3C3D triple-effect cycle. In particular, the condensed refrigerant from the third condenser (after being used to heat the second desorber), can be further used to heat the first desorber (by sub-cooling the condensed refrigerant). This ability to "double-couple" the third refrigerant flow to heat both the second and the first desorbers leads logically to naming these cycles "Double-Coupled-Condenser" or "Double-Condenser-Coupled" triple-effect cycles (DCC).

Although the energy available from this third refrigerant flow (sensible heat from the already condensed refrigerant) is small compared to the second refrigerant flow (heat of condensation from the refrigerant vapor), the resulting improvement in performance and practicality is significant.

There are two distinctly different methods for accomplishing this heat exchange. One method involves adding a separate heat exchanger to provide heat to the first generator by subcooling the third condensed refrigerant (Miyoshi et al, 1985). This DCC cycle utilizing a separate subcooler heat exchanger is shown in Figure 2. As can be seen in Figure 2, the subcooled refrigerant is shown as departing from the pure water refrigerant line at high pressure

before the then subcooled liquid is mixed with condensed refrigerant from the second condenser and/or the first condenser.

The second method for accomplishing the DCC triple-effect involves mixing the condensed third refrigerant from the third condenser with the refrigerant vapor from the second desorber, then using the combined second and third refrigerant flow to heat the first desorber (DeVault and Grossman, 1992; DeVault and Biermann, 1993). This DCC Triple-Effect cycle using the combined second and third refrigerant flow is shown in Figure 3. This cycle is labeled DCCA for convenience.

LiBr/H2O TRIPLE-EFFECT CYCLE DIAGRAMS

One may question why the diagram in Figure 3 is used to represent the DCCA Triple-Effect cycle rather than the diagram in Figure 1. Reasons why Figure 3 is preferred for the DCCA triple-effect cycle, rather than Figure 1, follow.

In the 3C3D triple-effect cycle, the condensed refrigerant from the third condenser goes to the evaporator without exchanging heat with the first desorber. This third refrigerant, having left the third condenser at (essentially) equilibrium goes to the evaporator without any additional heat exchange (eg: remaining at equilibrium). One can choose to mix or not mix the various condensed refrigerant flows going to the evaporator at any point, without departing from the pure refrigerant equilibrium line. Figure 1 correctly shows the 3C3D cycle.

Since Figure 1 clearly is the correct representation of the 3C3D triple-effect cycle, and is also consistent with the "PTX" diagrams used for decades to represent the identical condenser to evaporator refrigerant process for single-effect and double-effect cycles, what diagram should be used to represent the DCCA triple-effect cycle?

The actual thermodynamic and physical process for the DCAA cycle (when the third and second refrigerant flows are mixed) can not be precisely drawn on a 2-dimensional chart, since the 2-D chart does not show the changed refrigerant liquid-vapor composition.

Figure 4 shows a likely machine schematic for the DCCA cycle. As shown in Figure 4, in a real DCCA absorption chiller, the condensed refrigerant from the third condenser would be physically added to the refrigerant vapor from the second desorber before (or while) entering the second condenser heat exchanger. This mixing would occur at the outlet temperature of the second desorber, before heat was removed in the second condenser. This is clearly indicated by the Figure 3.

Since Figure 1 correctly shows the 3C3D triple-effect cycle, and since Figure 3 clearly shows all the fundament elements of the DCAA

Triple-Effect cycle by showing the physical process of mixing the second and third refrigerant streams before heating the first generator, Figure 3 is preferred.

METHODOLOGY OF SIMULATION

A modular computer code for simulation of absorption systems (ABSIM) was used to investigate the performance of the cycles under study. The code, developed specifically for flexible cycle simulation, has been described in detail by Grossman and Wilk (1992) and in a related report (Grossman, Gommed and Gadoth, 1991) containing a user's manual. The modular structure of the code makes it possible to simulate a variety of absorption systems in varying cycle configurations and with different working fluids. The code is based on unit subroutines containing the governing equations for the system's components and on fluids property subroutines containing thermodynamic properties of the working fluids. The components are linked together by a main program which calls the unit subroutines according to the user's specifications to form the complete cycle. When all the equations for the entire cycle have been established, a mathematical solver routine is employed to solve them simultaneously. The code is user-oriented and requires a relatively simple input containing the given operating conditions and the working fluid at each state point. The user conveys to the computer an image of the cycle by specifying the different components and their interconnections. Based on this information, the code calculates the temperature, flow rate, concentration, pressure and vapor fraction at each state point in the system and the heat duty at each unit, from which the coefficient of performance may be determined. The code has been employed successfully to simulate a variety of single-effect, double-effect and dual-loop absorption chillers, heat pumps and heat transformers employing the working fluids LiBr-H_2O, H_2O-NH_3, LiBr/$ZnBr_2$-CH_3OH, NaOH-H_2O and others. Recently, the same code was used to simulate the rather complex Generator-Absorber Heat Exchange (GAX) cycle employing ammonia-water, in several cycle variations.

The simulation methodology in the present study has followed an approach taken in earlier studies of single- and double-effect cycles (Gommed and Grossman, 1990) . Since the performance of each system depends on many parameters, the approach taken in all the simulation work has been to establish a design point for the system, and vary the relevant parameters around the design point. In particular, a performance map of COP and cooling capacity as functions of desorber heat supply temperature was generated for each system. Thus, the performance of systems in single, double and triple stages could be compared not only at a single point but over the entire temperature domain applicable to the cycle.

The system's performance under a given set of operating conditions depends on the design characteristics and particularly on the size of the heat transfer surfaces in its exchange units – the

evaporators, absorbers, condensers, desorbers, etc. As a reference case for comparing the different LiBr/H2O triple-effect cycles, a practical system was considered with economically reasonable, if not optimized, heat transfer areas. In the earlier study of simpler systems (Gommed and Grossman, 1990) a reference case was selected based on the heat exchanger performance of a single-effect solar-powered liBr/H2O chiller known as SAM-15 (Biermann, 1978) that has been extensively tested. A three-condenser-three-desorber (3C3D) triple-effect LiBr/H2O chiller in series flow type 1 (according to Figure 5) with SAM-15 size evaporator, absorber, condensers, desorbers and recuperators, and with SAM-15 flows of the external fluids is used as a reference triple-effect case. Selecting the reference case in this manner made it possible to use the results of the present triple-effect cycles simulation for comparison with those of the simpler, single- and double-effect cycles (Gommed and Grossman, 1990), on an equivalent basis. The design characteristics of the triple-effect reference system are listed in Table 1, including the external flow rates of cooling and chilled water; the weak absorbent circulation rate; the UA's (overall heat transfer coefficient times area), which characterize the heat transfer performance of the exchange units; and design point temperatures of the external fluids and of the solution outlet from the gas-fired desorber (for this desorber the external fluid loop is redundant). With these values as input, the simulation code calculates the internal temperatures, flow rates, concentrations, and other operating parameters at all the system's state points from which overall performance parameters were calculated.

Properties of liBr/H2O for the simulation were taken from the ASHRAE Handbook (1985). The thermodynamic property equations were extrapolated, where necessary, to the high temperature range required by the triple-effect cycles. The amount of extrapolation required was relatively moderate for the 3C3D, DCC and DCCA cycles considered.

CYCLE ANALYSIS

The purpose of the present study has been to simulate the various LiBr/H2O triple-effect cycles in detail and compare their performances to each other. Specifically, systems based on the LiBr/H2O triple-effect chiller cycles mentioned above have been compared to each other on an equivalent basis and also to single-effect and double-effect systems using the same size components. Another goal of the study has been to investigate the effect of specific design parameters on the cycles' performance. Some parametric analysis has been conducted which indicates performance trends.

Figure 5 describes schematically the ABSIM components and state points for the three-condenser-three-desorber (3C3D) triple-effect liBr/H2O chiller, forming an extension of the conventional double-

effect cycle. The system has 16 components or sub-units (indicated by the circled numbers) and 42 state points (indicated by the uncircled numbers). The first Absorber (2) and first condenser (5) are externally cooled; the third desorber (13) is externally heated. Chilled water is produced in evaporator (1). Heat rejected from the second condenser (6) powers the first desorber (3) and heat from the third condenser (14) powers the second desorber (4). The coupling between each condenser-desorber pair is through a circulating heat transfer fluid loop, as shown, but may also be achieved by physically combining the two components, such that the refrigerant condensing on one side of a heat exchange surface would heat the solution desorbing on the other side of that surface. The absorbent solution is in a series flow arrangement shown in Figure 5 (Gommed and Grossman, 1990). This flow arrangement, termed a series flow type 1, normally requires three solution pumps with the entire amount of weak solution flowing from the absorber to the first desorber, continuing to the second desorber, then to the third desorber and back to the absorber. A series flow type 2 (not shown) is also possible, with the weak solution from the absorber going first to the third desorber, continuing to the second and then to the first desorber before returning to the absorber. This arrangement may be achieved with one solution pump. According to simulation results of double-effect cycles (Gommed and Grossman, 1990) the two series flow arrangements yield very similar performance results.

Figure 6 describes the same cycle in parallel flow, where the weak solution from the absorber is split and divided among the three desorbers. This system has 17 components and 47 state points, counting the extra flow mixers, but is identical in hardware to the system of Figure 1 except for the parallel flow piping arrangement. According to simulation results of double-effect cycles (Gommed and Grossman, 1990), the parallel flow arrangement is superior in performance to the series flow in terms of increased COP and a reduced risk of crystallization.

Figure 7 describes a triple-effect Double-Condenser-Coupled (DCC) triple-effect chiller in series flow type 1. The system has 17 components and 44 state points and is very similar to the one in Figure 4. In comparison to the 3C3D cycle, it includes an additional recuperative heat exchanger (17) which subcools the hot condensate leaving the third condenser (14) and rejects the heat to first desorber (3) via the circulation loop 10-11-44. This heat exchanger transfers a modest amount of heat, compared to all other units in the cycle. An additional benefit for this heat recuperation is in providing extra cooling capacity to the evaporator through the now subcooled refrigerant, at no additional expenditure of high grade heat. An added benefit is a somewhat increased generation capacity of the first desorber (3). Figure 8 shows the same triple-effect DCC system in a parallel flow arrangement. The system has 18 components and 49 state points. As evident from Figure 7, the difference between this and the series

flow system is that the weak solution from the absorber is divided at certain fractions among the three desorbers, each receiving only the amount it is supposed to regenerate.

The DCCA cycle is shown in Figure 9. The system shown is in parallel flow and is very similar to the one in Figure 7 without the recuperator (17). The heat recuperation from the hot condensate and the beneficial subcooling effect associated with it is achieved by discharging the condensate from third condenser (14) into the cooler second condenser (6), and similarly, discharging the condensate from condenser (6) into the cooler first condenser (5). As will be shown later, this system performs better than the one in Figure 8 and requires one less heat exchanger. This system may be configured in series flow as well.

The parallel flow of Figure 6 differs from the system in Figure 5 only by the piping arrangement. This holds true also for the DCC systems in Figures 7 and 8 which contain, however, an additional small heat exchanger (17). This heat exchanger transfers a modest amount of heat, compared to all other units, and it alone has been characterized in all the calculations in terms of a closest approach temperature (CAT) of 5°F. Thus, the set of operating parameters in Table 1 has been selected as the design point for the above DCC and DCCA cycles in addition to the reference 3C3D system of Figure 5. For the parallel flow systems (Figures 6, 8 and 9), an equal distribution of the weak solution among the three desorbers has been selected at the design point, that is, the flow rates at state points 8, 13, and 33 are 20.0 lbs/min each.

RESULTS OF SIMULATION

In conducting the simulation to generate the operating curves of the above systems, the solution outlet temperature from the third gas-fired desorber (13) (state point 37) was varied while all the other parameters were kept constant. It was assumed that the values of the UA for the exchange units remain constant while the temperatures and all the other parameters change. In reality, this is not strictly accurate; although the heat transfer areas (A) remain constant, the heat transfer coefficients (U) vary somewhat with the temperatures as well as with the loading conditions. However, this variation is relatively weak in most cases and the assumption of constant UA is a reasonably good approximation. Better fundamental understanding of the combined heat and mass transfer process in absorption and desorption would allow taking the variation of UA with temperature into consideration.

The coefficient of performance (COP) of the different cycles has been defined as the ratio of the heat quantity in the evaporator producing the desired cooling effect, to that supplied to the externally heated third desorber. For LiBr/H2O absorption chillers, the effect of solution pumping and other parasitic losses is small, and is not considered in this study.

Figure 10 describes the COP of the reference 3C3D triple-effect series flow type 1 system (Figure 5) as a function of the heat supply temperature to the externally heated desorber (13), for different cooling water inlet temperatures, and for a fixed chilled water outlet temperature. The curves for the single-effect SAM-15 and for a series flow type 1 double-effect system with SAM-15 size components, are also plotted for comparison. The single-effect and double-effect curves were taken from simulations conducted under the earlier study of Gommed and Grossman (1990) using the same code. The design point for each system is indicated by a dot. The COP of the ideal Carnot cycle operating under the same conditions is also included for comparison. It is evident that all systems exhibit the same typical, qualitative behavior, with the COP increasing sharply from zero at some minimum temperature, then levelling off to some constant value at a higher temperature and even decreasing slightly with further increase in temperature. The reason for this behavior is well understood and is explained in detail in other references (Gommed and Grossman, 1990). The 3C3D triple-effect system has a COP higher than the single- and double-effect cycles but requires a higher minimum heat supply temperature in order to begin operating. For all three systems, the COP is closest to Carnot in the "knee" of the curve and levels off as the heat supply temperature increases. The single-effect system gives best results in the heat supply temperature range of 150-220°F. Above that, from an efficiency point of view, it is beneficial to switch to the double-effect system, which performs best at the heat supply temperature range of 220-300°F. With a still higher heat supply temperature, a triple-effect system is more desirable.

Figure 11 describes the COP for the five cycles in Figures 5, 6, 7, 8 and 9, as a function of the heat supply temperature to the externally heated desorber (13), for fixed values of the design cooling water inlet temperature (85°F) and chilled water outlet temperature (45°F). The typical behavior of the COP increasing sharply from zero at some minimum temperature and then levelling off to some constant value at higher temperatures, is clearly observed here. As expected, the two DCC systems with a condensate subcooler (Figures 7 and 8) show a higher COP than their 3C3D counterparts (Figures 5 and 6). In each category, the parallel flow system yields better performance than the series flow. The best performance is exhibited by the parallel flow DCCA system of Figure 9. In comparing the series flow DCC with the series flow 3C3D cycle, the following trend is observed. At low temperatures the COP curves for the two cycles approach each other, with no advantage to the DCC. With increasing temperature, the value of subcooling the refrigerant becomes more significant, resulting in a higher COP of the DCC than the 3C3D. The same trend is valid for the three parallel flow systems.

A definite advantage for the parallel flow systems is evident over those with series flow. The main reason for this is that in the series flow systems, the entire amount of absorbent solution passes

through all three desorbers, whereas in the parallel flow systems each desorber receives only the amount of solution it needs to regenerate. This reduces circulation losses considerably. The same trend is evident in double-effect systems (Gommed and Grossman, 1990). Another advantage of the parallel flow system is in reduced concentration at the absorber inlet (state point 1) which reduces the risk of crystallization. In the series flow systems the high concentration solution generated at the third desorber (13) flows to the absorber while cooling down. In the parallel flow systems the same solution is diluted on its way to the absorber and its concentration is lowered by mixing with solution streams from the lower temperature desorbers (3) and (4). For comparison, the design point concentration of the strong LiBr-H_2O solution at the absorber inlet (state point 1) is 64.1% for the series flow DCC (Figure 7) and only 63.0% for the parallel flow DCC (Figure 8).

The solution flow rate distribution among the three desorbers in the parallel flow systems (Figures 6, 8 and 9) has been selected equal at the design point. However, an equal distribution of solution is not necessarily optimal. Based on the simulation of double-effect systems (Gommed and Grossman, 1990), an improvement may be gained by deviating from an equal distribution both in increasing the COP and reducing the risk of crystallization. Here, the effect of varying the solution flow to the three desorbers has been investigated for the parallel flow DCCA system of Figure 9, operating otherwise at the design condition. Figure 12 shows the COP of the DCCA system as a function of the solution flow to the second desorber (state point 13) for different values of the flow to the third desorber (state point 33). The rest of the design solution flow (totalling 60 lbs/min) goes to the first desorber (state point 8). In the extreme cases where either of the three desorbers is starved for solution, the entire system goes out of balance and both the COP and capacity tend to zero. As evident from Figure 12, the improved distribution of solution to the third, second and first desorbers are approximately 10, 10 and 40 lbs/min, respectively. Under this condition, the COP reaches 1.83, instead of 1.73 at equal distribution; the solution concentration at the absorber inlet (state point 1) is reduced to 60.5%, compared to 62.9% at equal distribution. The capacity is reduced somewhat due to the lower concentration, as explained in the previous paragraph. Note that the improved flow distribution at the design temperatures is not necessarily preserved in off-design conditions.

Further optimization may be possible. Note that some unit size mismatch exists in the 3C3D and DCC reference systems. A constrained optimization study is in order, where the COP of the various cycles would be maximized under a requirement for a fixed cooling capacity, fixed heat supply temperatures and fixed total UA (or properly weighed total UA) of the system. The optimizer will select the optimal distribution of UA among the system's components and select the optimum solution flow. This is the subject of

another study.

CONCLUSION

Performance simulation has been carried out for several LiBr/H2O triple-effect cycles, including the Three-Condenser-Three-Desorber (3C3D) and Double-Condenser-Coupled (DCC and DCCA) configurations. A common reference condition was established for the LiBr/H2O triple-effect cycles based on the component sizes and flow rates of the single-effect SAM-15 system. Performance simulation was carried out over a range of operating conditions, including some investigation of the influence of the design parameters. COP's ranging from 1.27 for the series-flow 3C3D to 1.73 for the parallel flow DCCA have been calculated at the design point. Further improvement in the DCCA cycle to a 1.83 COP was calculated by varying flow rates to the desorbers.

The DCC and DCCA cycles constitute an improvement over the corresponding 3C3D cycles, which may be obtained at essentially no additional cost through a different piping arrangement. In each category, the parallel flow system yields a better COP than the series flow, with a lower risk of crystallization, but with slightly reduced capacity. An optimization study should be carried out in order to fully determine these cycles potential.

ACKNOWLEDGEMENT

This work has been supported in part under Oak Ridge National Laboratory Subcontract 80X-SK033V.

REFERENCES

Alefeld, G., 1982:"Regeln fur den Entwurf von Mehrstufigen Absorbermaschinen" (Rules for the Design of Multistage Absorption Machines), Brennst-Warme-Kraft, Vol. 34, pp. 64-73.

Alefeld, G., 1983a: "Double Effect, Triple-Effect and Quadruple Effect Absorption Machines", *Proceedings, XVIth International Congress of Refrigeration*, Paris, France, pp. 951-956.

Alefeld, G., 1983b: "Design Optimization For Multi-stage compression, expansion and absorption devices", *Proceedings, XVIth International Congress of Refrigeration*, Paris, France, pp. 9-14.

Alefeld, G., and Ziegler, F. 1985a: "Advanced Absorption Cycles", *Proceedings, Absorption Heat Pumps Congress*, Paris, France, March 20-22, C11, pp. 159-164.

Alefeld, G., 1985b: "Multi-stage apparatus having working fluid and absorption cycles, and method of operation thereof." U.S. Patent 4,531,372, July 30.

Alefeld, G., and Radermacher, R. 1993: "Heat Conversion Systems", Textbook published by CRC Press

ASHRAE Handbook of Fundamentals, 1985 : Thermodynamic Properties of Lithium Bromide-Water. pp. 17.69-17.70.

Biermann, W. J., 1978: "Prototype energy retrieval and solar system, Bonneville Power Administration", *Proceedings, 3rd Workshop on the Use of Solar Energy for Cooling of Buildings*, San Francisco, CA, pp. 29-34. Also personal communication regarding Carrier SAM-15 solar-powered water-lithium bromide absorption chiller, July 1986.

DeVault, R.C., 1988: "Triple-effect absorption chiller utilizing two refrigerant circuits". U.S. Patent 4,732,008, March 22.

DeVault, R.C. and Biermann, W.J., 1989: "Seven-effect absorption refrigeration". U.S. Patent 4,827,728, May 9.

DeVault, R.C. and Marsala, J., 1990a: "Ammonia-water triple-effect absorption cycle". ASHRAE paper No. AT-90-27-1, presented at the ASHRAE 1990 Winter Meeting, Atlanta, GA, February 10-14.

DeVault, R.C., 1990b: "Triple-Effect Absorption Chiller Cycle: A Step Beyond Double-Effect Cycles", IEA Heat Pump Centre: Proceedings of the Workshop on High Performance Heat Pumps, Wider Market Applications and Market, Susono City, Japan, pp. II-27-40, March 9-10.

DeVault, R.C. and Biermann, W.J., 1992a: "Triple-effect absorption refrigeration system with double-condenser coupling". U.S. Patent 5,205,136, April 27.

DeVault, R.C. and Grossman, G., 1992b: "Triple-effect absorption chiller cycles". Presented at the International Gas Research Conference IGRC92, Orlando, Florida, November 16-19.

Gommed, K. and Grossman, G., 1990: "Performance analysis of staged absorption heat pumps: Water-lithium bromide systems". ASHRAE paper No. AT-90-30-6, presented at the 1990 ASHRAE Winter Meeting, Atlanta, GA, February 10-14.

Grossman, G., K. Gommed and D. Gadoth, 1987: "A computer model for simulation of absorption systems in flexible and modular form," ASHRAE paper No. NT-87-29-2, presented at the 1987 ASHRAE Annual Meeting, Nashville, TN, June 27-July 1.

Grossman, G. and Wilk, M., 1992: "Advanced modular simulation of absorption systems". Presented at the 1992 ASME Winter Annual Meeting, Anaheim, CA, November 8-13.

Kurosawa, S., 1988: "Current Status of Gas Air-Conditioning System

in Japan", Tokyo Gas Co. Ltd., paper presented at the Advanced Absorption Workshop, Oak Ridge, Tennessee, October 4.

Miyoshi, N., Sugimoto, S. and Aizawa, M., 1985: "Multi-Effect Absorption Refrigerating Machine", U.S. Patent 4,551,991, November 12.

Oouchi, T., Usui, S., Fukuda, T. and Nishiguchi, A., 1985: "Multi-Stage Absorption Refrigeration System". U.S. Patent 4,520,634, June 4.

Whitlow, E.P., and Swearingen, J.S., 1958: "An Improved Absorption Refrigeration Cycle", paper presented at the 13th Annual Technical Meeting, South Texas Section, American Institute of Chemical Engineers, Galveston, Texas, October 3.

Whitlow, E.P. 1993: Personal communication, July 28.

Wilkinson, W.H. 1987: "What Are The Performance Limits For Double-Effect Absorption Cycles?" ASHRAE Transactions, Vol. 93, Part 2.

Ziegler, F., Brandl, F., Volkl, J. and Alefeld, G. 1985: "A Cascading Two-Stage Sorption Chiller System Consisting of a Water-Zeolite High Temperature Stage and a Water-LiBr Low Temperature Stage". *Proceedings, the Absorption Heat Pumps Congress,* Paris, France, March 20-22, pp. 231-238.

Ziegler, F., and Alefeld, G., 1987: "Coefficient of Performance of Multistage Absorption Cycles", International Journal of Refrigeration, Vol 10, pp. 285-295, September.

Ziegler, F., Kahn, R., Summerer F., and Alefeld, G., 1993: "Multi-effect absorption chillers" International Journal of Refrigeration, September 1993.

TABLE 1

Characteristic Parameters at Design Point for 3C3D, DCC and DCCA Triple-Effect LiBr-H_2O Absorption Chillers

Heat Transfer Characteristics (UA):	
Absorber:	193.0 Btu/min. °F
Desorbers:	268.0 Btu/min. °F
Condensers:	565.0 Btu/min. °F
Evaporator:	377.0 Btu/min. °F
Recuperative Heat Exchangers:	64.0 Btu/min. °F
Mass Flow Rates:	
Absorber (cooling water)	483.0 lbs/min
Low Temperature Condenser (cooling water)	391.0 lbs/min
Evaporator (chilled water)	300.0 lbs/min
Internal Coupling Water Loops, 10-11 and 15-16	400.0 lbs/min
Weak Solution	60.0 lbs/min
Temperatures:	
Hot solution outlet from gas-fired desorber (13) (s.p. 37)	425°F
Cooling water inlet (s.p. 3 and 23):	85°F
Chilled water outlet (s.p. 29)	45°F

LIST OF FIGURES

Figure 1: Diagram of the three-condenser-three-desorber (3C3D) triple-effect chiller

Figure 2: Diagram of the double-condenser-coupled (DCC) triple-effect chiller using a separate subcooler heat exchanger

Figure 3: Diagram of alternate double-condenser-coupled (DCCA) triple-effect chiller using combined refrigerant flow

Figure 4: Possible machine design for DCAA triple-effect cycle

Figure 5: ABSIM schematic description of three-condenser-three-desorber (3C3D) triple-effect chiller in series flow

Figure 6: ABSIM schematic description of three-condenser-three-desorber (3C3D) triple-effect chiller in parallel flow

Figure 7: ABSIM schematic description of double-condenser-coupled (DCC) triple-effect chiller in series flow

Figure 8: ABSIM schematic description of double-condenser-coupled (DCC) triple-effect chiller in parallel flow

Figure 9: ABSIM schematic description of alternate double-condenser-coupled (DCCA) triple-effect chiller in parallel flow

Figure 10: Coefficient of Performance for single-effect (dashed lines), double-effect series flow (solid lines) and 3C3D triple-effect series flow (dot-dashed lines) systems as functions of operating temperatures. Carnot COP for the same operating conditions is given by the dotted lines.

Figure 11: Coefficient of Performance for DCC, DCCA and 3C3D triple-effect cycles as a function of the heat supply temperature to the high temperature desorber.

Figure 12: Coefficient of Performance for the parallel flow DCCA cycle as a function of the solution flow distribution to the three desorbers.

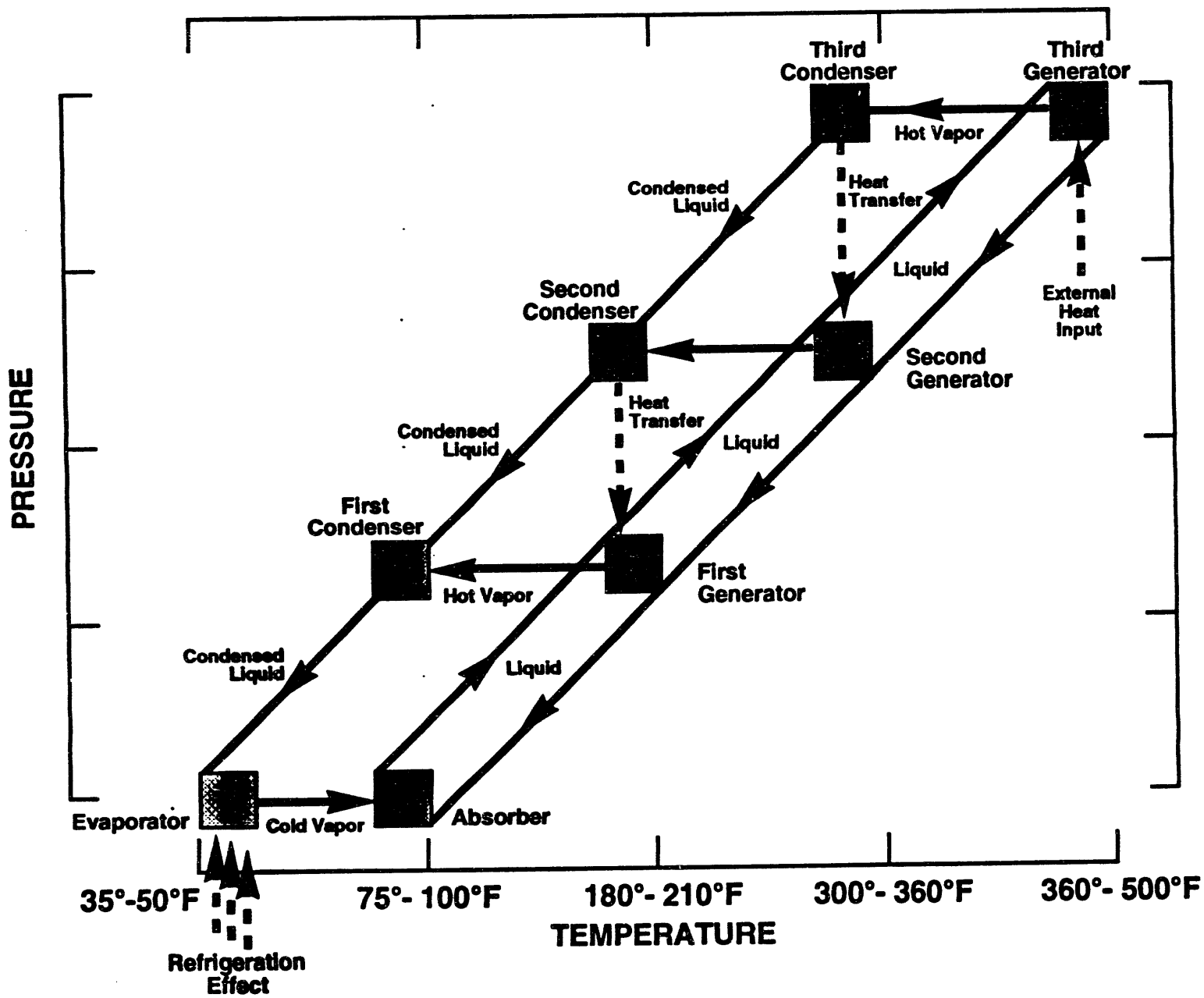

Figure 1: Diagram of the three-condenser-three-desorber (3C3D) triple-effect chiller

DOUBLE CONDENSER COUPLED TRIPLE-EFFECT CYCLE

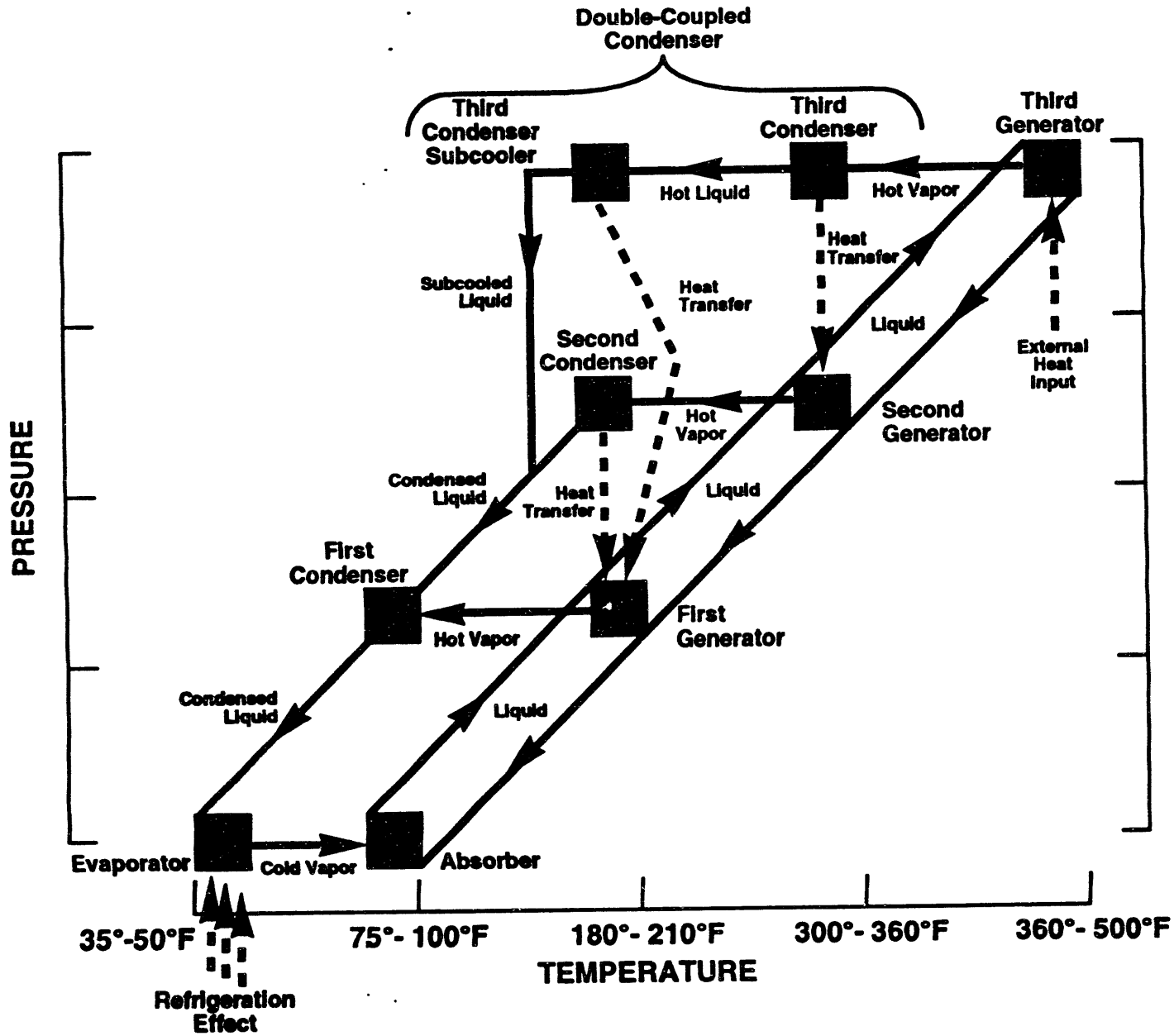

Figure 2: Diagram of the double-condenser-coupled (DCC) triple-effect chiller using a separate subcooler heat exchanger

ORNL-DWG 94M-5059

DOUBLE CONDENSER COUPLED TRIPLE-EFFECT CYCLE

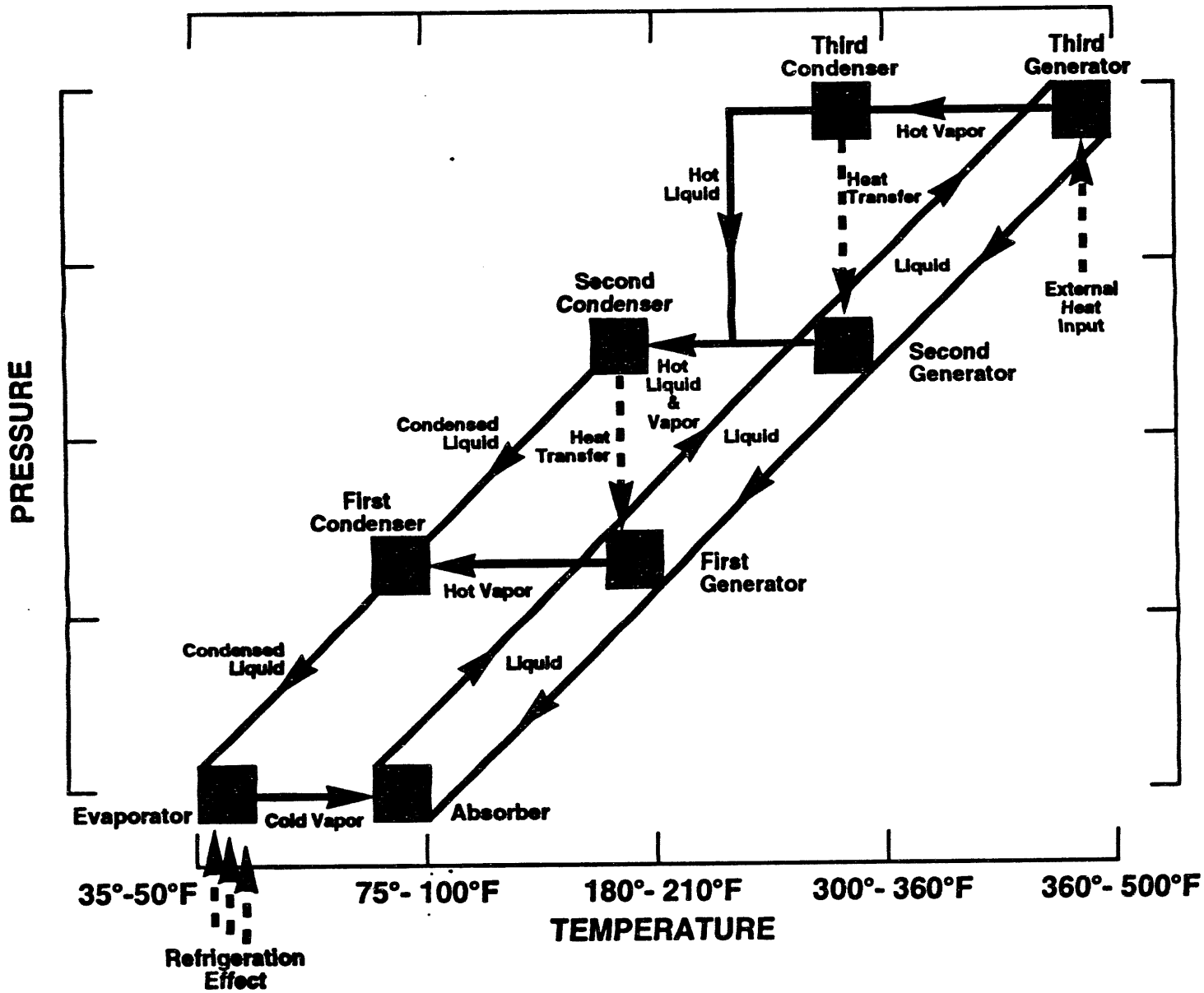

Figure 3: Diagram of alternate double-condenser-coupled (DCCA) triple-effect chiller using combined refrigerant flow

ORNL-DWG 94M-5058

DCC APPARATUS

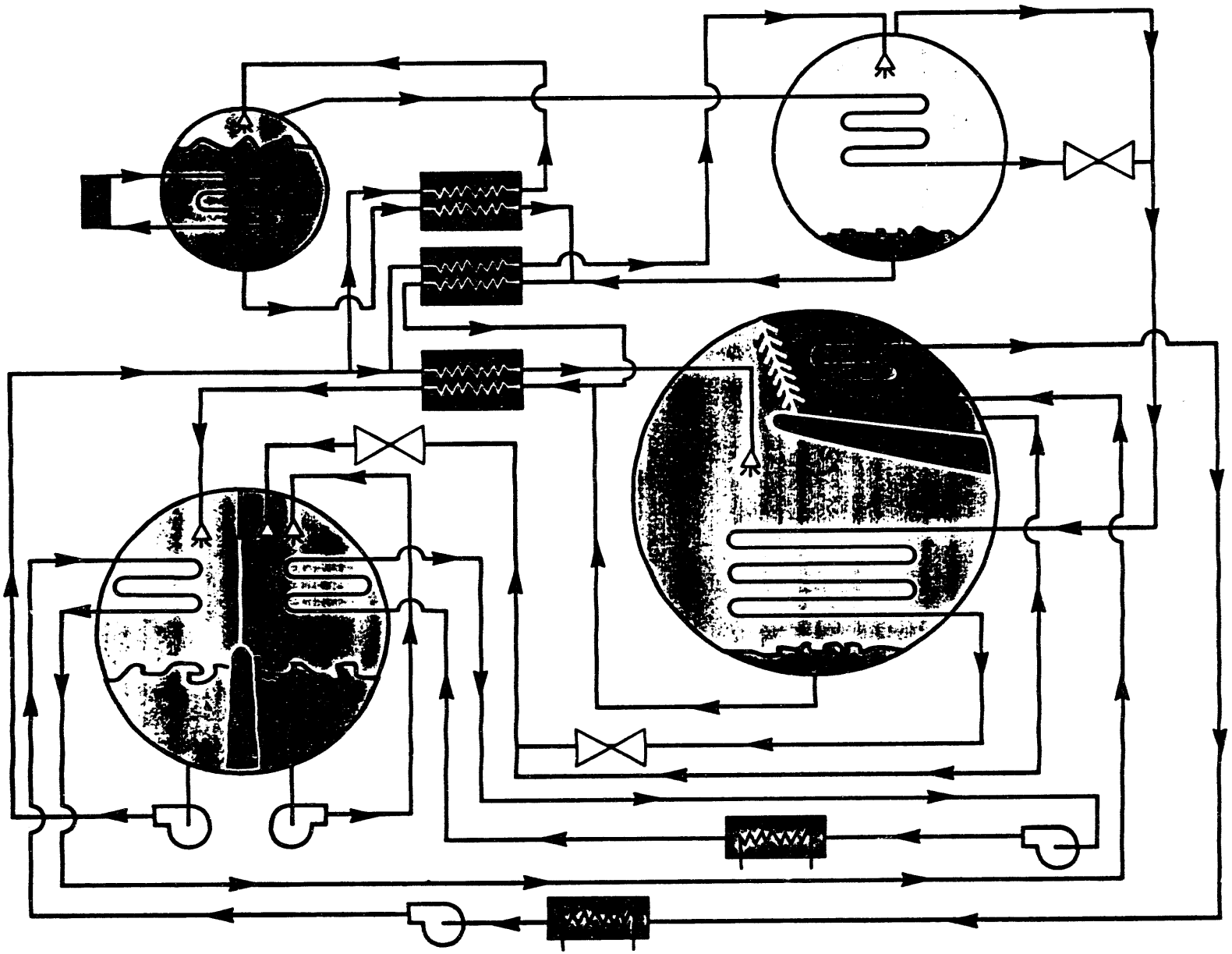

Figure 4: Possible machine design for DCAA triple-effect cycle

ORNL-DWG 93M-16654

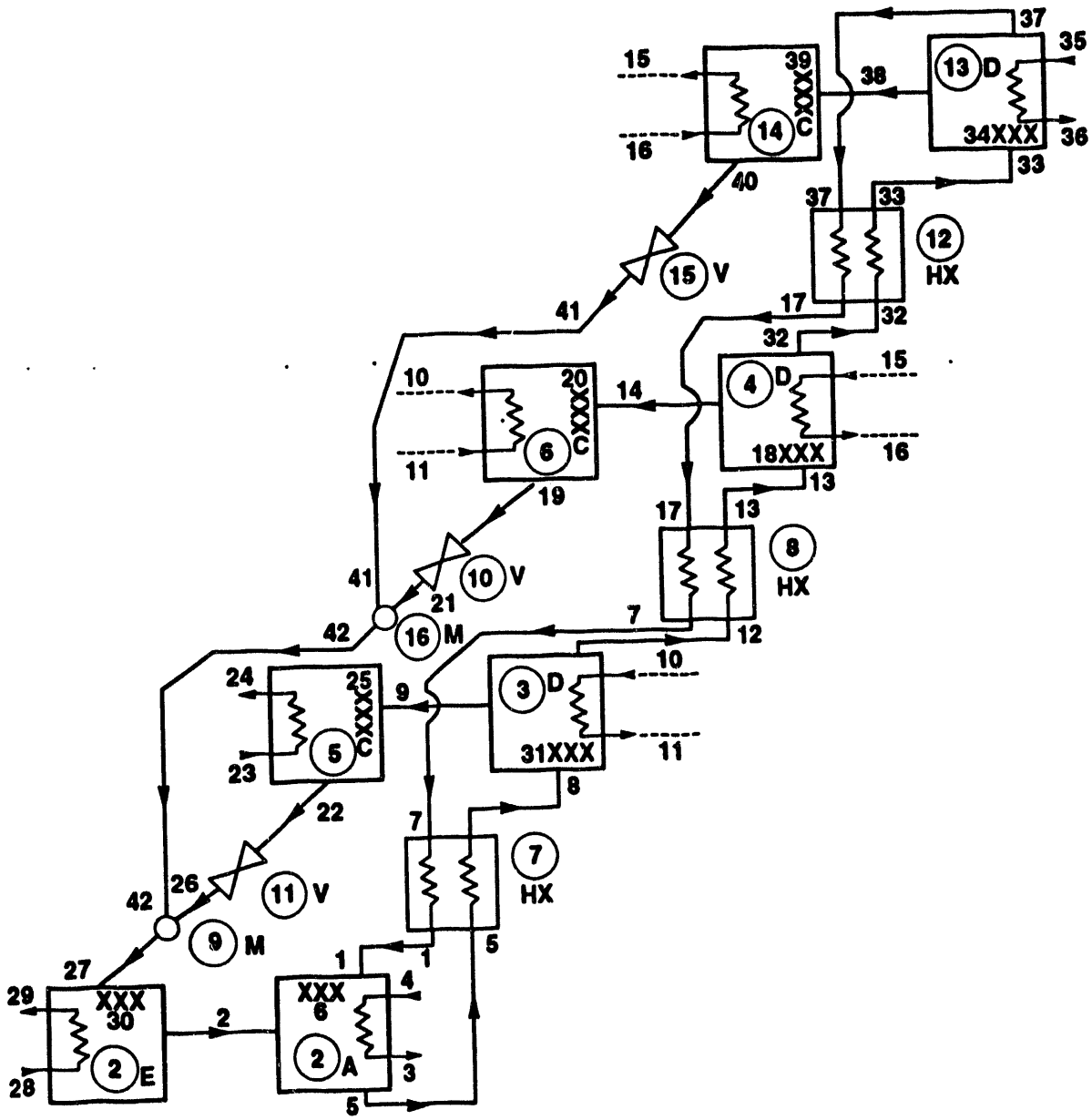

Figure 5: ABSIM schematic description of three-condenser-three-desorber (3C3D) triple-effect chiller in series flow

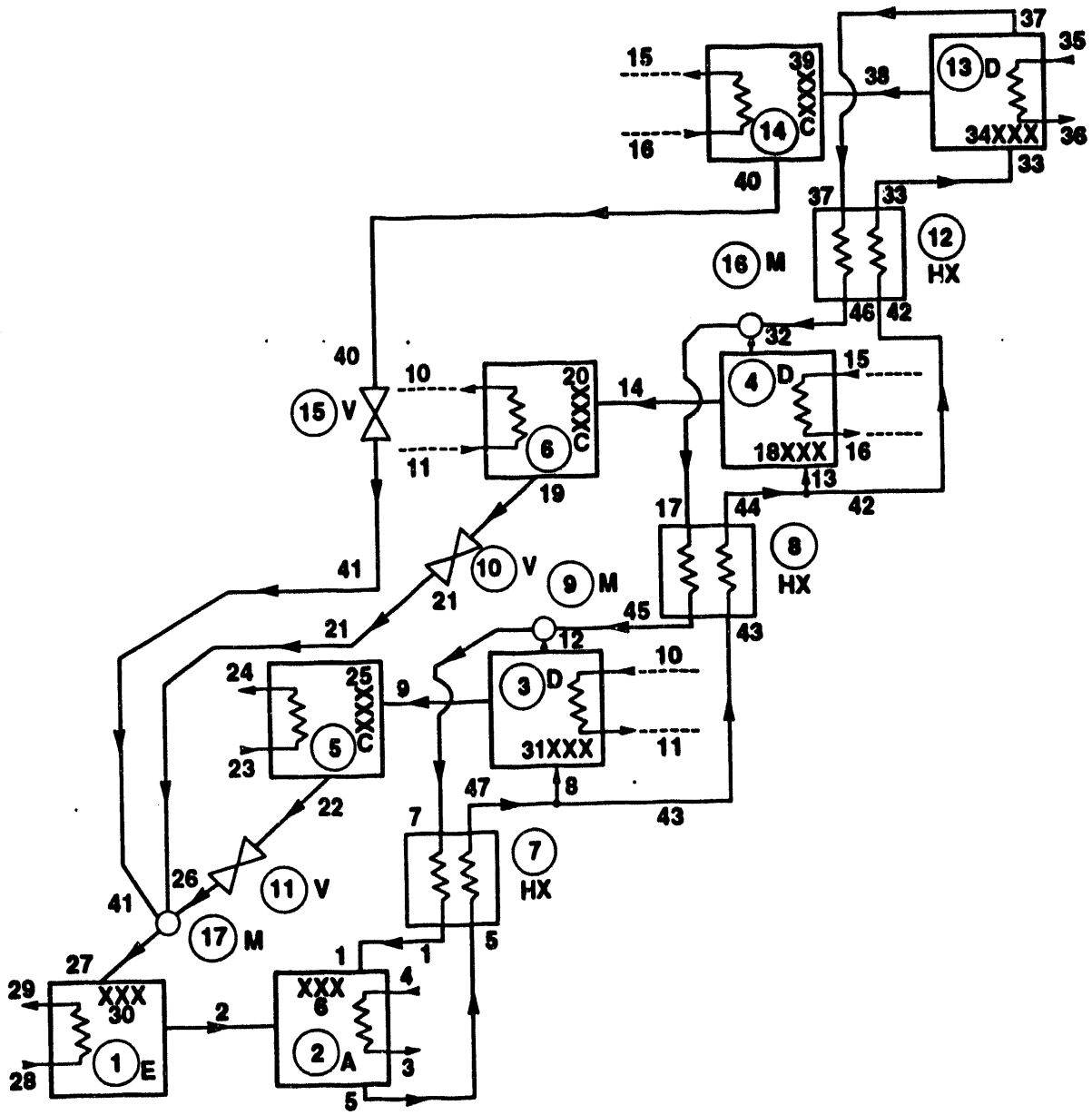

Figure 6: ABSIM schematic description of three-condenser-three-desorber (3C3D) triple-effect chiller in parallel flow

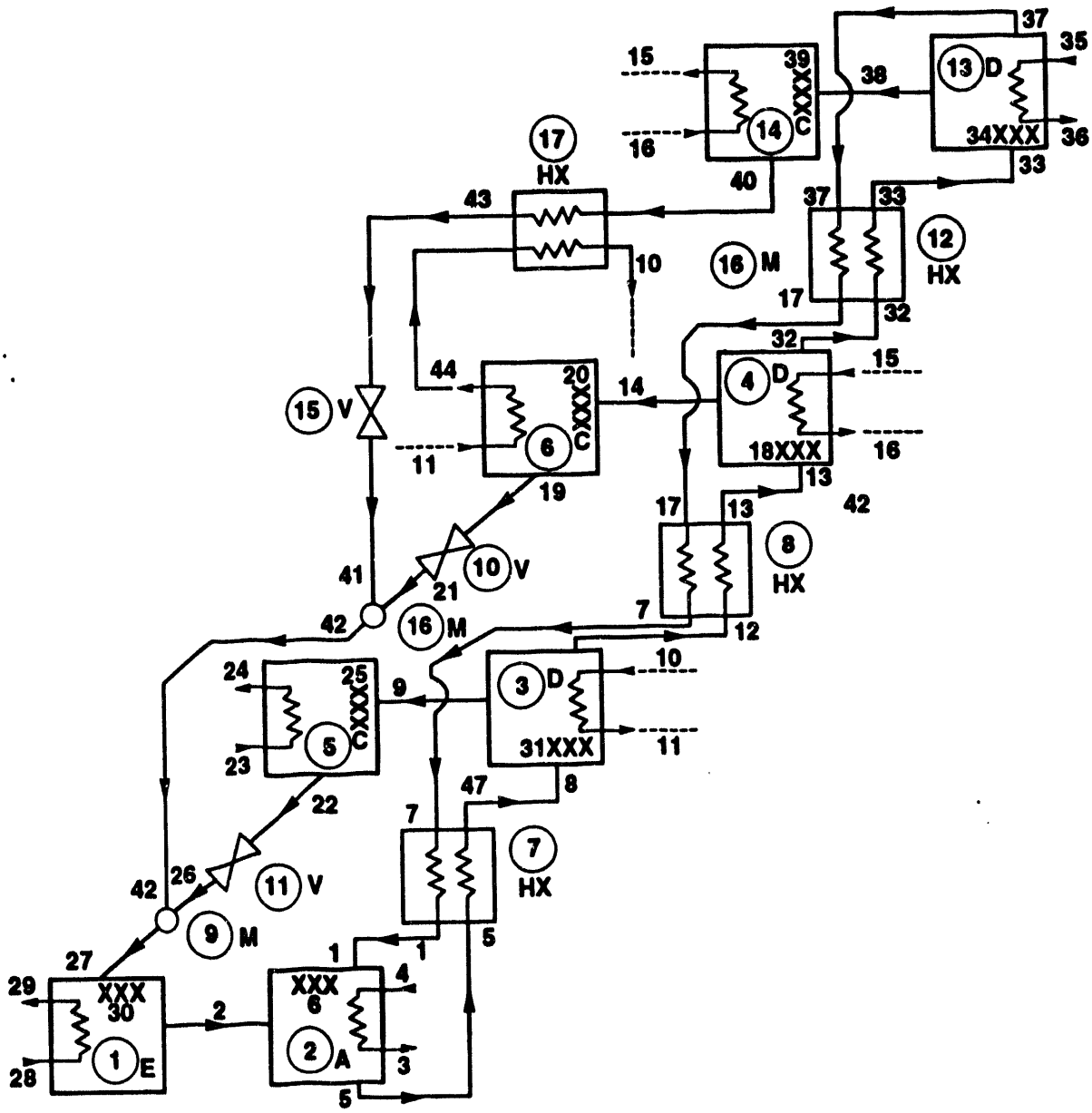

Figure 7: ABSIM schematic description of double-condenser-coupled (DCC) triple-effect chiller in series flow

ORNL-DWG 93M-16657

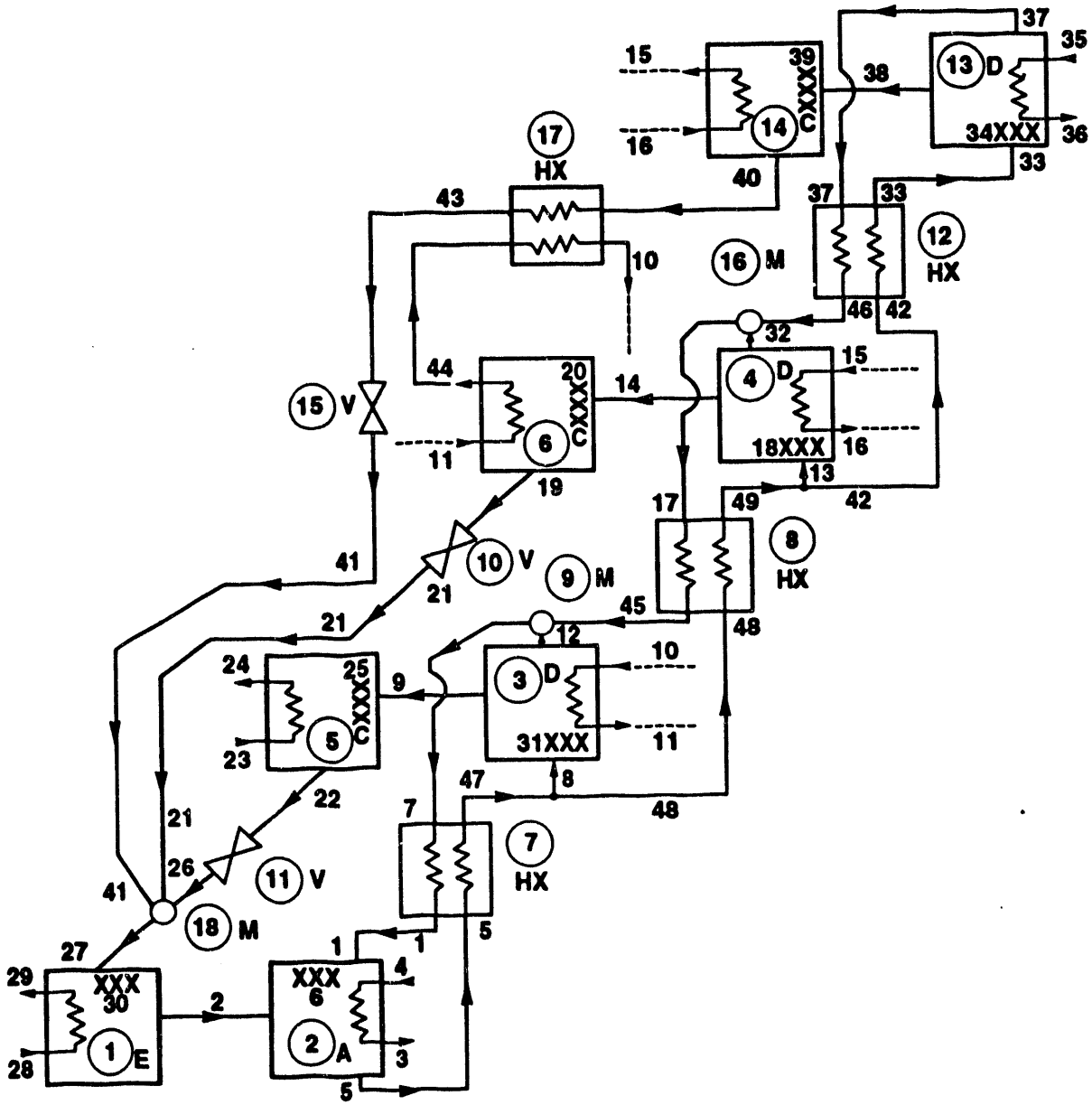

Figure 8: ABSIM schematic description of double-condenser-coupled (DCC) triple-effect chiller in parallel flow

ORNL-DWG 93M-16658

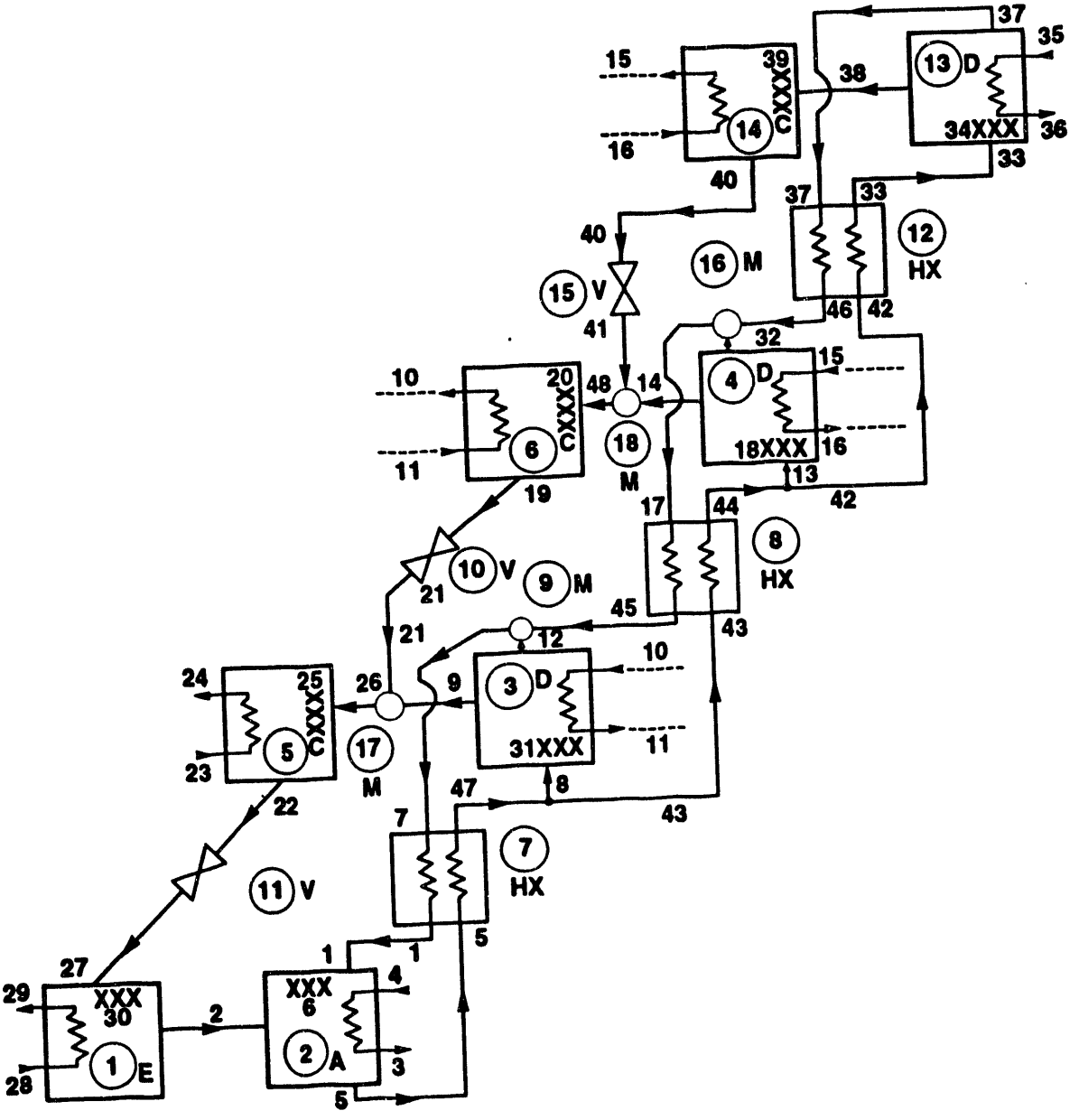

Figure 9: ABSIM schematic description of alternate double-condenser-coupled (DCCA) triple-effect chiller in parallel flow

ORNL-DWG 93M-16660

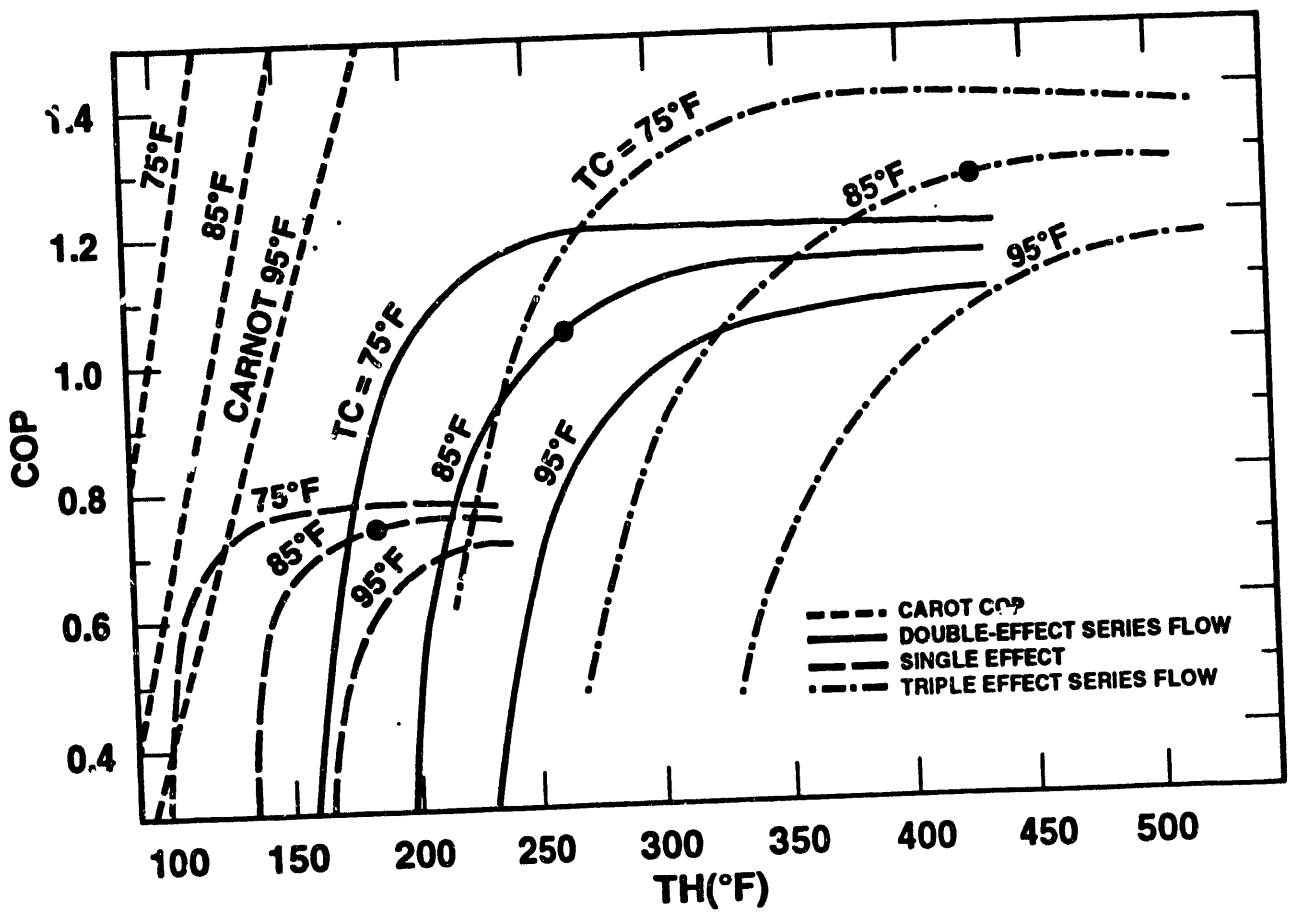

Figure 10: Coefficient of Performance for single-effect (dashed lines), double-effect series flow (solid lines) and 3C3D triple-effect series flow (dot-dashed lines) systems as functions of operating temperatures. Carnot COP for the same operating conditions is given by the dotted lines.

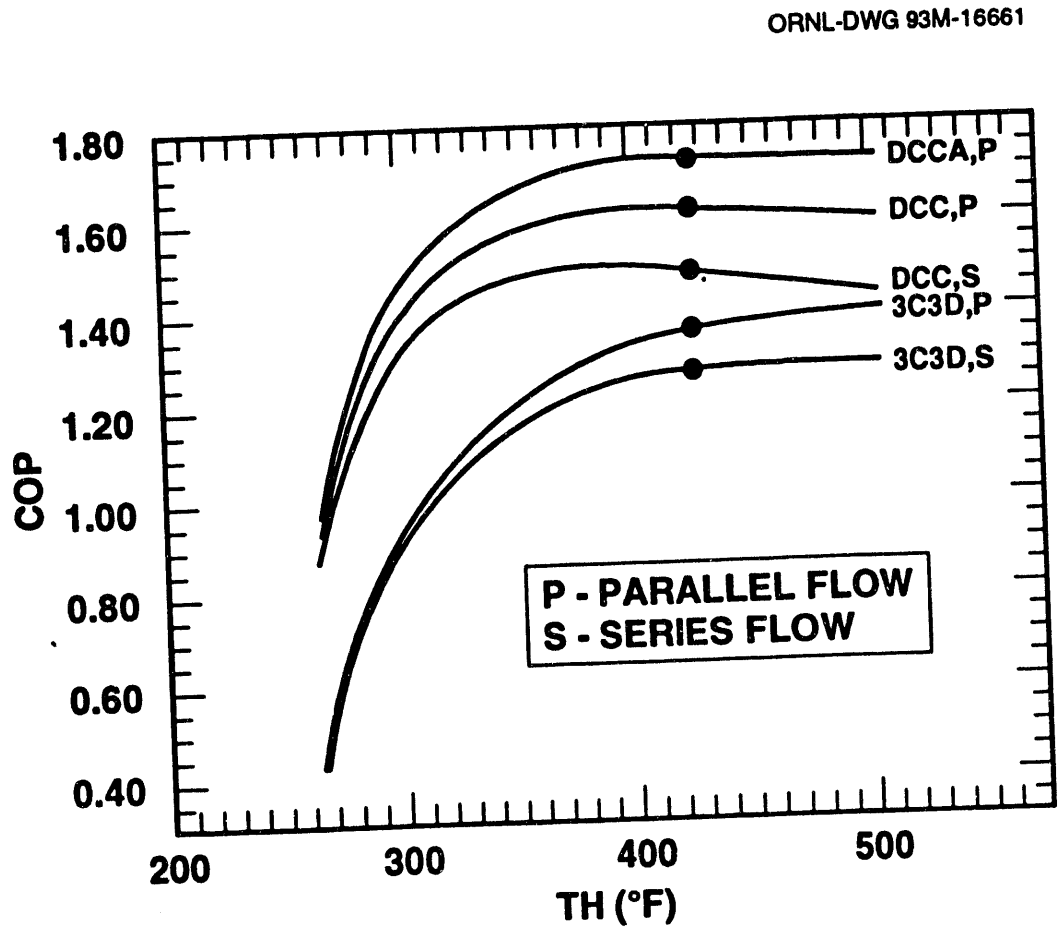

Figure 11: Coefficient of Performance for DCC, DCCA and 3C3D triple-effect cycles as a function of the heat supply temperature to the high temperature desorber.

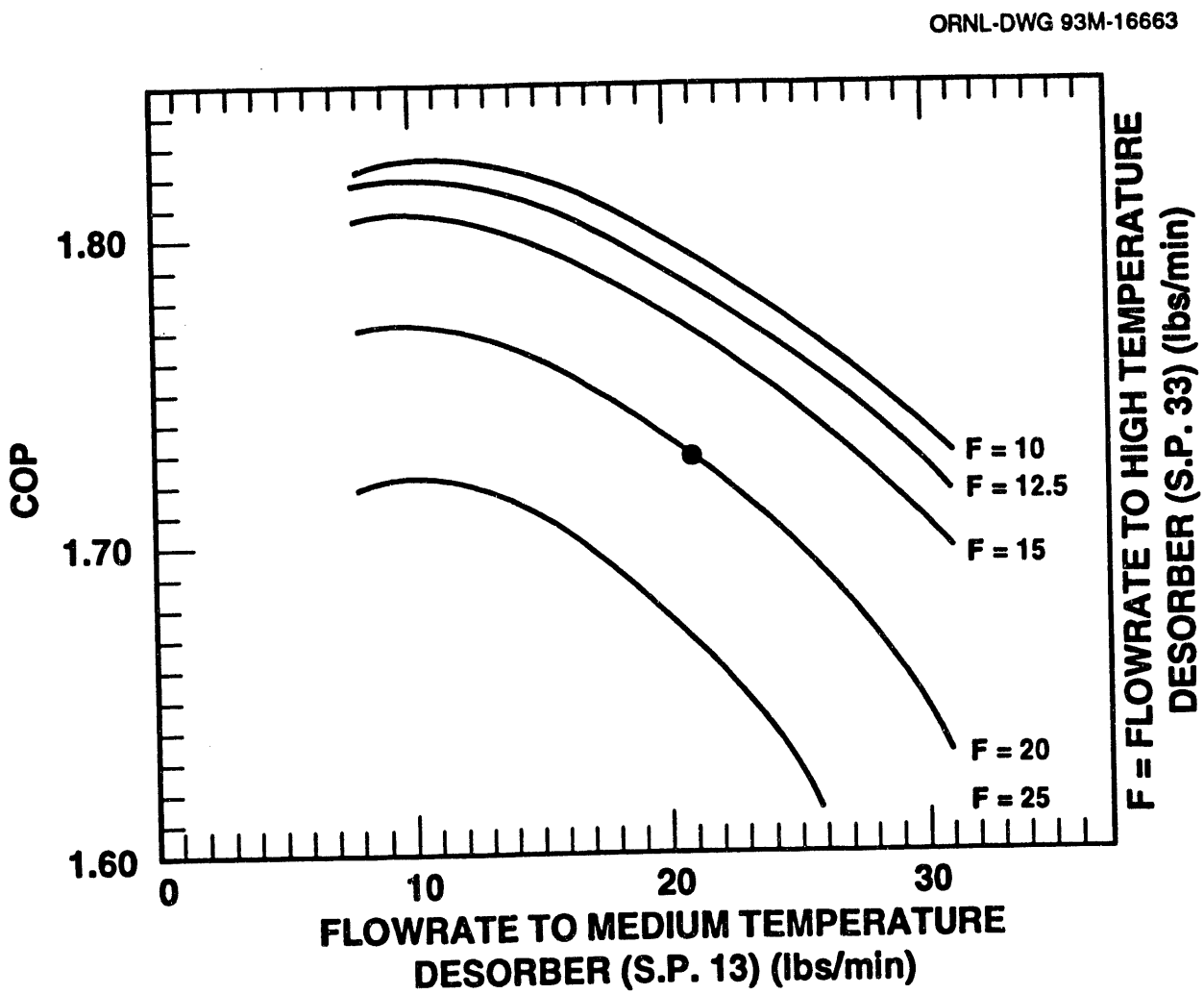

Figure 12: Coefficient of Performance for the parallel flow DCCA cycle as a function of the solution flow distribution to the three desorbers.

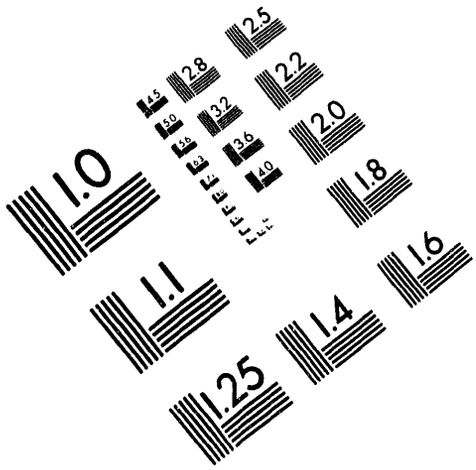

Association for Information and Image Management
1100 Wayne Avenue, Suite 1100
Silver Spring, Maryland 20910
301/587-8202

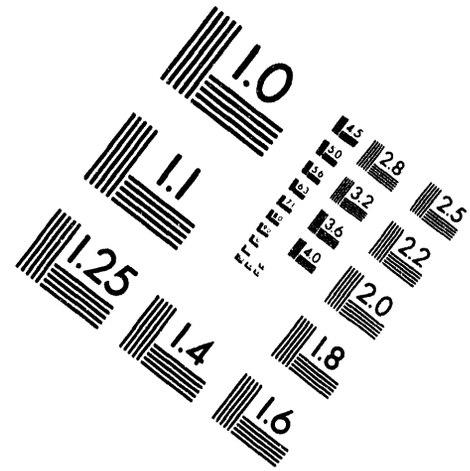

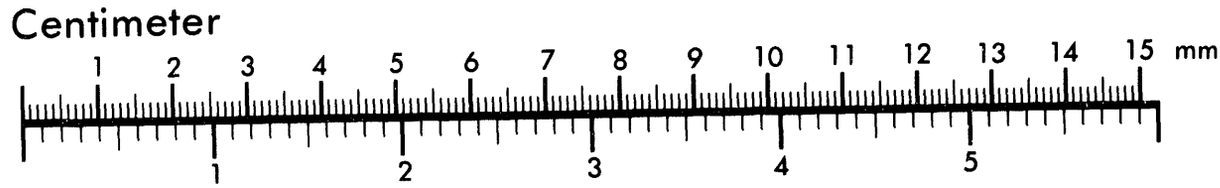

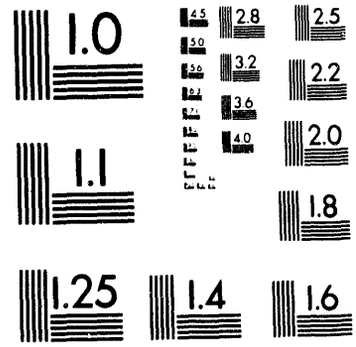

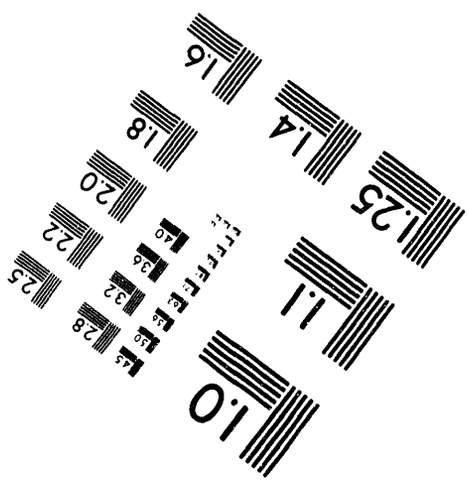

MANUFACTURED TO AIIM STANDARDS
BY APPLIED IMAGE, INC.

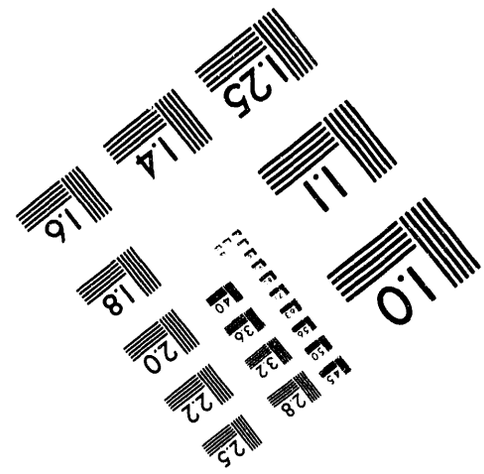

DATE
FILMED
12/15/94

END